Physics Letters B 768 (2017) 180–186

Contents lists available at ScienceDirect

Physics Letters B

www.elsevier.com/locate/physletb

The effect of chemical potential on imaginary potential and entropic force

Zi-qiang Zhang [a,*], De-fu Hou [b], Gang Chen [a]

[a] School of mathematics and physics, China University of Geosciences (Wuhan), Wuhan 430074, China
[b] Institute of Particle Physics and Key Laboratory of Quark and Lepton Physics (MOS), Central China Normal University, Wuhan 430079, China

ARTICLE INFO

Article history:
Received 30 December 2016
Accepted 22 February 2017
Available online 28 February 2017
Editor: M. Cvetič

ABSTRACT

Imaginary potential and entropic force represent different mechanisms for melting the heavy quarkonium. In this paper, we study the chemical potential effect on these two quantities with respect to a moving quarkonium from the AdS/CTF duality. We observe that for both mechanisms the chemical potential has the same effect: the presence of the chemical potential tends to decrease the dissociation length.

1. Introduction

The experiments of heavy ion collisions at LHC and RHIC have produced a new state of matter so-called "strong quark-gluon plasma (sQGP)" [1–3]. One main experimental signatures for sQGP formation is melting of quarkoniums, such as J/ψ and excited states, in the medium [4]. It was argued earlier [5] that the color screening is the main mechanism responsible for this suppression. But recently some other mechanisms, such as the imaginary potential [6,7] and the entropic force [8] have been proposed. AdS/CFT [9–11], the duality between a string theory in AdS space and a conformal field theory in the physical space-time, has yielded many important insights for studying strongly coupled field theory. This method has been used to study the imaginary potential and the entropic force recently.

The imaginary potential can be used to estimate the width of heavy quarkonia in plasma. Also, it can yield to the suppression of the $Q\bar{Q}$ in heavy ion collisions. By using the AdS/CFT duality, J. Noronha et al. have carried out the imaginary potential for $\mathcal{N}=4$ SYM theory in their seminal work [12]. There, the $\mathrm{Im}V_{Q\bar{Q}}$ is related to the effect of thermal fluctuations due to the interactions between the heavy quarks and the medium. Soon the investigations of [12] have been extended to various cases. For instance, the imaginary potential of static quarkonium in strongly coupled plasma is discussed in [13,14]. The $\mathrm{Im}V_{Q\bar{Q}}$ of moving quarkonium in strongly coupled plasma has been studied in [15]. The finite 't Hooft coupling corrections on this quantity is analyzed in [16]. Other important results can be found, for example, in [17–19]. In addition, there are other approaches which can also extract an imaginary part of the potential from the holography [20,21].

Another important quantity related to the suppression of $Q\bar{Q}$ is the entropic force. This force has been introduced long time ago [22] and proposed to responsible for the gravity recently [23]. In a more recent work, D. E. Kharzeev [8] show that the entropic force is responsible for dissociating the quarkonium. This argument is based upon the Lattice QCD results that a large amount of entropy related to the heavy quarkonium placed in the QGP [24–26]. Applying the AdS/CFT, K. Hashimoto et al. have studied the entropic force associated with the heavy quark pair firstly [27]. It is shown that the peak of the entropy near the transition point associates with the nature of deconfinement. After [27], the entropic force of a moving heavy quarkonium has been studied in [28], it is found that the velocity leads to increasing the entropic force thus making the moving quarkonium dissociates easier. We have investigated the entropic force of a rotating heavy quarkonium in [29] and observed that the rotating quarkonium dissociates harder than the static case.

As we know, the $Q\bar{Q}$ pair is not produced at rest in sQGP. Therefore, the effect of the medium in motion of $Q\bar{Q}$ should be taken into account. In this paper, we will investigate the chemical potential effect on the imaginary potential as well as the entropic force with respect to a moving quarkonium in plasma from AdS/CFT. We would like to see how the chemical potential affects the two quantities or the quarkonium dissociation. Moreover, imaginary potential and entropic force represent different mechanisms for the melting of the heavy quarkonium, so it would be

* Corresponding author.
E-mail addresses: zhangzq@cug.edu.cn (Z.-q. Zhang), houdf@mail.ccnu.edu.cn (D.-f. Hou), chengang1@cug.edu.cn (G. Chen).

http://dx.doi.org/10.1016/j.physletb.2017.02.055

interesting to compare them. Evaluations of the chemical potential effect on these two quantities could be considered as a simple text of this "comparison". These are the main motivations of the present work.

We organize the paper as follows. In the next section, we briefly review the AdS Schwarzchild background with chemical potential and boost the frame in one direction. In section 3, we study the imaginary potential of a moving quarkonium in this background and discuss the effect of the chemical potential on it. The chemical potential effect on the entropic force with respect to a moving quarkonium in the same background will be investigated in section 4. The last section is devoted to conclusion and discussion.

2. Setup

In the holographic dictionary, $\mathcal{N}=4$ SYM theory with a chemical potential can be obtained by making the black hole in the holographic dimension be charged. The corresponding spacetime is the AdS_5-Reissner–Nordstrom geometry. The metric is given by

$$ds^2 = -\frac{r^2}{R^2}f(r)dt^2 + \frac{r^2}{R^2}d\vec{x}^2 + \frac{R^2}{r^2}f(r)^{-1}dr^2, \tag{1}$$

with

$$f(r) = 1-(1+Q^2)(\frac{r_h}{r})^4 + Q^2(\frac{r_h}{r})^6, \tag{2}$$

where R is the AdS space radius, r denotes the radial coordinate with $r=r_h$ the horizon. The string tension is $\frac{1}{2\pi\alpha'}$ where α' is related to the 't Hooft coupling constant by $\frac{R^2}{\alpha'}=\sqrt{\lambda}$.

The temperature is

$$T = \frac{r_h}{\pi R^2}(1-\frac{Q^2}{2}), \tag{3}$$

with the restriction $0\le Q\le\sqrt{2}$ for the charge Q of the black hole.

The chemical potential μ is given by

$$\mu = \frac{\sqrt{3}Q r_h}{R^2}. \tag{4}$$

Note that in the limit $\mu\to 0$, the usual AdS_5-Schwarzschild metric is reproduced, as expected.

However, we should admit that the chemical potential implemented in this way is not the quark (or baryon) chemical potential of QCD but a chemical potential which is conjugate to an R-charge associated with supersymmetry [30]. As it indeed behaves like a chemical potential, one can use it as a simple way of introducing the finite density effects into the system.

Next, to make the quark-antiquark pair moving, we assume that the plasma is at rest and the frame is moving in one direction. Here we boost the frame in the x_3 direction with rapidity β so that

$$\begin{aligned} dt &= dt' cosh\beta - dx_3' sinh\beta,\\ dx_3 &= -dt' sinh\beta + dx_3' cosh\beta. \end{aligned} \tag{5}$$

Substituting (5) into (1) and dropping the primes, we have the boosted metric as

$$\begin{aligned} ds^2 =& [-\frac{r^2}{R^2}f(r)cosh^2\beta + \frac{r^2}{R^2}sinh^2\beta]dt^2\\ &- 2sinh\beta cosh\beta[\frac{r^2}{R^2} - \frac{r^2}{R^2}f(r)]dtdx_3\\ &+ [-\frac{r^2}{R^2}f(r)sinh^2\beta + \frac{r^2}{R^2}cosh^2\beta]dx_3^2\\ &+ \frac{r^2}{R^2}(dx_1^2+dx_2^2) + \frac{R^2}{r^2}f(r)^{-1}dr^2. \end{aligned} \tag{6}$$

3. Imaginary potential

In this section, we follow the calculations of [12] to analyze the imaginary potential with the metric (6). Generally, to investigate the moving quarkonium, one should consider different alignments for the quarkonium with respect to the plasma wind, including parallel ($\theta=0$), transverse ($\theta=\pi/2$), or arbitrary direction (θ). In this paper, we discuss the two extreme cases: $\theta=0$ and $\theta=\pi/2$.

We now consider the system parallel to the wind in the x_3 direction, the coordinate is parameterized by

$$t=\tau,\qquad x_1=0,\qquad x_2=0,\qquad x_3=\sigma,\qquad r=r(\sigma). \tag{7}$$

In this case, the quarks are located at $x_3=-\frac{L}{2}$ and $x_3=\frac{L}{2}$, where L is the inter-distance between the $Q\bar{Q}$.

To proceed, the Nambu–Goto action is

$$S = -\frac{1}{2\pi\alpha'}\int d\tau d\sigma\,\mathcal{L} = -\frac{1}{2\pi\alpha'}\int d\tau d\sigma\sqrt{-g}, \tag{8}$$

here g is the determinant of the induced metric with

$$g_{\alpha\beta} = g_{\mu\nu}\frac{\partial X^\mu}{\partial\sigma^\alpha}\frac{\partial X^\nu}{\partial\sigma^\beta}, \tag{9}$$

where $g_{\mu\nu}$ is the metric, X^μ is the target space coordinates. σ^α parameterize the world sheet with $\alpha=0,1$.

From (6) and (7), we have the induced metric

$$\begin{aligned} g_{00} &= \frac{r^2}{R^2}f(r)cosh^2\beta - \frac{r^2}{R^2}sinh^2\beta,\\ g_{11} &= \frac{r^2}{R^2}cosh^2\beta - \frac{r^2}{R^2}f(r)sinh^2\beta + \frac{R^2}{f(r)r^2}\dot{r}^2, \end{aligned} \tag{10}$$

with $\dot{r}=dr/d\sigma$.

Then the lagrangian density can be written as

$$\mathcal{L} = \sqrt{a(r)+b(r)\dot{r}^2}, \tag{11}$$

where

$$\begin{aligned} a(r) =& \frac{r^4}{R^4}[f(r)sinh^4\beta + f(r)cosh^4\beta\\ &- sinh^2\beta cosh^2\beta(1+f^2(r))],\\ b(r) =& cosh^2\beta - \frac{1}{f(r)}sinh^2\beta. \end{aligned} \tag{12}$$

As the action does not depend on σ explicitly, the solution satisfies

$$\mathcal{L} - \frac{\partial\mathcal{L}}{\partial\dot{r}}\dot{r} = constant. \tag{13}$$

The deepest point of the U-shaped string is $r=r_c$ with $\dot{r}=0$, one gets

$$\dot{r} = \frac{dr}{d\sigma} = \sqrt{\frac{a^2(r)-a(r)a(r_c)}{a(r_c)b(r)}}, \tag{14}$$

with

$$\begin{aligned} a(r_c) =& \frac{r_c^4}{R^4}[f(r_c)sinh^4\beta + f(r_c)cosh^4\beta\\ &- sinh^2\beta cosh^2\beta(1+f^2(r_c))],\\ f(r_c) =& 1-(1+Q^2)(\frac{r_h}{r_c})^4 + Q^2(\frac{r_h}{r_c})^6. \end{aligned} \tag{15}$$

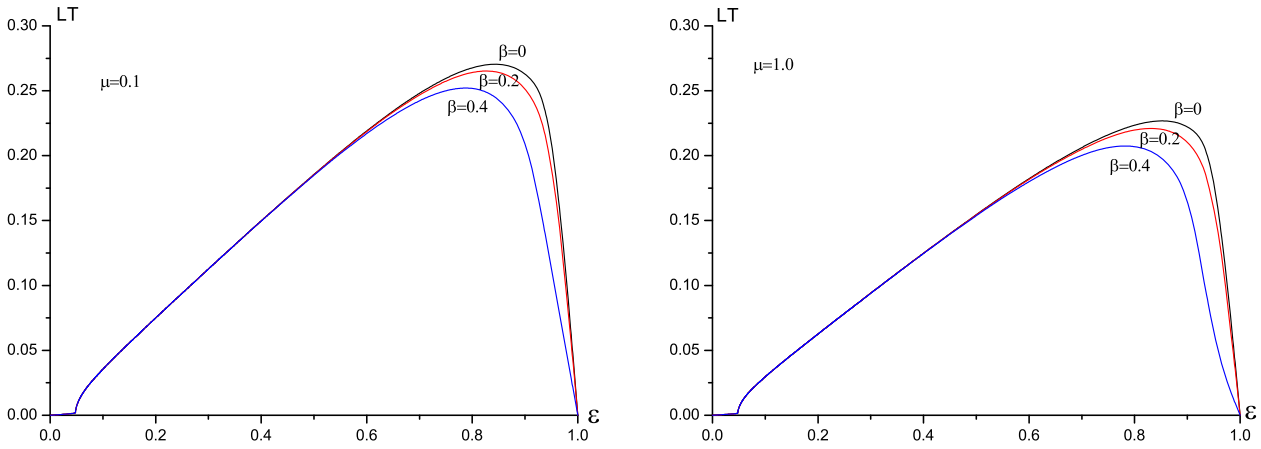

Fig. 1. LT versus ε for $\theta = 0$. Left: $\mu = 0.1$. Right: $\mu = 1$. In all of the plots from top to bottom $\beta = 0, 0.2, 0.4$ respectively.

Integrating (14), one finds the separate length of the $Q\bar{Q}$ as

$$L = 2\int_{r_c}^{\infty} dr \sqrt{\frac{a(r_c)b(r)}{a^2(r) - a(r)a(r_c)}}. \tag{16}$$

The real part of the heavy quark potential can be derived from the classical solution of the equations of motion

$$ReV_{Q\bar{Q}} = \frac{1}{\pi\alpha'}\int_{r_c}^{\infty} dr[\sqrt{\frac{a(r)b(r)}{a(r) - a(r_c)}} - \sqrt{b(r_0)}] - \frac{1}{\pi\alpha'}\int_{r_h}^{r_c} dr\sqrt{b(r_0)}, \tag{17}$$

where $b(r_0) = b(r \to \infty)$.

The imaginary part of the heavy quark potential can be obtained by using the thermal worldsheet fluctuation method

$$ImV_{Q\bar{Q}} = -\frac{1}{2\sqrt{2}\alpha'}[\frac{a'(r_c)}{2a''(r_c)} - \frac{a(r_c)}{a'(r_c)}]\sqrt{b(r_c)}, \tag{18}$$

where the derivations are with respect to r. Note that one can recover the $\mathrm{Im}V_{Q\bar{Q}}$ of the moving quarkonium [15] by taking $\mu = 0$ in (18).

Now, we are ready to calculate the inter-distance and imaginary potential. From (3), (4) and (16), the resulting expression for LT can be written as

$$LT = 2\frac{r_h}{\pi R^2}(1 - \frac{(\frac{\mu R^2}{\sqrt{3}r_h})^2}{2})\int_{r_c}^{\infty} dr\sqrt{\frac{a(r_c)b(r)}{a^2(r) - a(r)a(r_c)}}. \tag{19}$$

In Fig. 1, we plot LT as a function of ε with $\varepsilon \equiv r_h/r_c$ for various cases. One can see that for each plot there is a maximum value of ε_{max}, and that LT is an increasing function of ε for $\varepsilon < \varepsilon_{max}$. On the other hand, for $LT > LT_{max}$, LT is a decreasing function of ε. Actually, in this case one needs to take into account new configurations [31] which are not solutions of the Nambu–Goto action. Here we consider only $LT < LT_{max}$.

In Fig. 1 we show LT versus ε for $\theta = 0$ of three different rapidity. The left panel of Fig. 1 is plotted for a small value of chemical potential ($\mu = 0.1$) while the right panel is for a larger value of chemical potential ($\mu = 1.0$). We can see that at a fixed μ increasing the rapidity leads to decreasing the LT_{max}. This result is in agreement with that in [15,16]. In addition, by comparing the left panel with the right panel, we can see that for each β as μ increases the LT_{max} decreases. In other words, the presence of the chemical potential tends to decrease the LT_{max}.

Then we calculate the imaginary potential from (18), after some algebra one finds

$$a'(r) = (sinh^4\beta + cosh^4\beta)(4r^3 f(r) + r^4 f'(r)) - sinh^2\beta cosh^2\beta(4r^3 + 4r^3 f^3(r) + 2r^4 f(r) f'(r)), \tag{20}$$

$$a''(r) = (sinh^4\beta + cosh^4\beta)(12r^2 f(r) + 8r^3 f'(r) + r^4 f''(r)) - sinh^2\beta cosh^2\beta(12r^2 + 12r^2 f^2(r) + 8r^3 f(r) f'(r) + 2r^4 f(r) f''(r) + 8r^3 f'(r) f(r) + 2r^4 f'(r) f'(r)), \tag{21}$$

with

$$f'(r) = 4(1 + Q^2)r_h^4 r^{-5} - 6Q^2 r_h^6 r^{-7},$$
$$f''(r) = -20(1 + Q^2)r_h^4 r^{-6} + 42Q^2 r_h^6 r^{-8}. \tag{22}$$

From (18), (20), (21) and (22), we can obtain the $ImV_{Q\bar{Q}}$. Numerically, we plot $ImV/(\sqrt{\lambda}T)$ against LT for $\theta = 0$ of three different rapidity in Fig. 2. For each plot we can see that the imaginary potential starts at a L_{min} which can be found by solving $ImV_{Q\bar{Q}} = 0$ and ends at a L_{max}. In addition, at a fixed chemical potential, by increasing the rapidity the absolute value of the imaginary potential decreases. Moreover, comparing the left panel with the right one, one finds increasing the chemical potential leads to decreasing the absolute value of the imaginary potential. In other words, turning on the chemical potential effect leads to generating the $ImV_{Q\bar{Q}}$ for smaller inter-quark distances. It was argued [12] that the imaginary potential can be used to estimate the thermal width of heavy quarkonium and in general a large thermal width corresponding to a large dissociation length. Thus, the chemical potential has the effect of decreasing the thermal width or decreasing the dissociation length. Interestingly, the higher derivative corrections has the similar behavior [16].

Next, we consider the system transverse to the wind in the x_1 direction. The parametrization is

$$t = \tau, \qquad x_1 = \sigma, \qquad x_2 = 0, \qquad x_3 = 0, \qquad r = r(\sigma). \tag{23}$$

here the quarks are located at $x_1 = -\frac{L}{2}$ and $x_1 = \frac{L}{2}$.

The next analysis is similar to the parallel case in the previous section. So we here focus on the results.

In Fig. 3, the LT versus ε for $\theta = \pi/2$ at two different chemical potential have been shown. In Fig. 4, the $ImV/(\sqrt{\lambda}T)$ against LT for $\theta = \pi/2$ at two different chemical potential are also presented. One finds that the results are very similar to the parallel

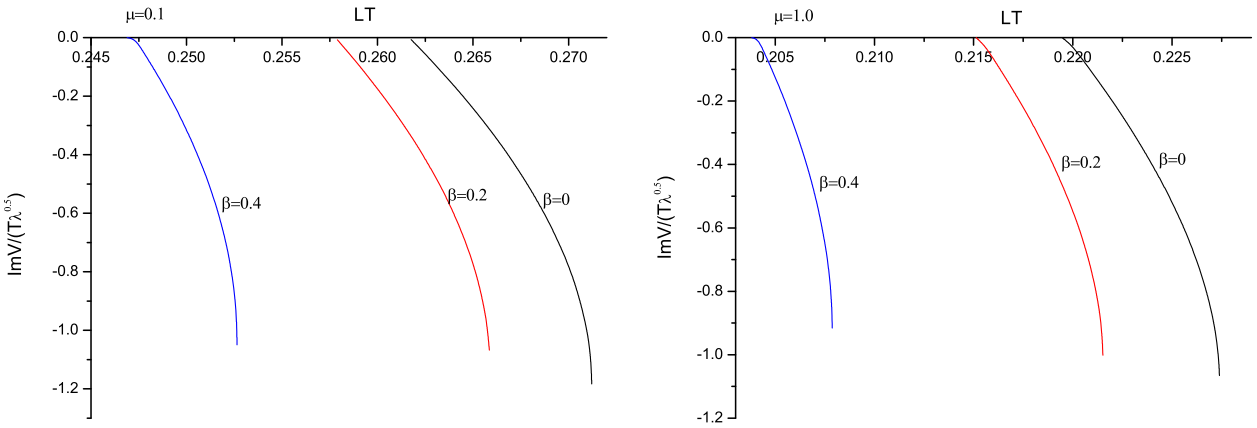

Fig. 2. $ImV/(\sqrt{\lambda}T)$ versus LT for $\theta = 0$. Left: $\mu = 0.1$. Right: $\mu = 1$. In all of the plots from left to right $\beta = 0.4, 0.2, 0$ respectively.

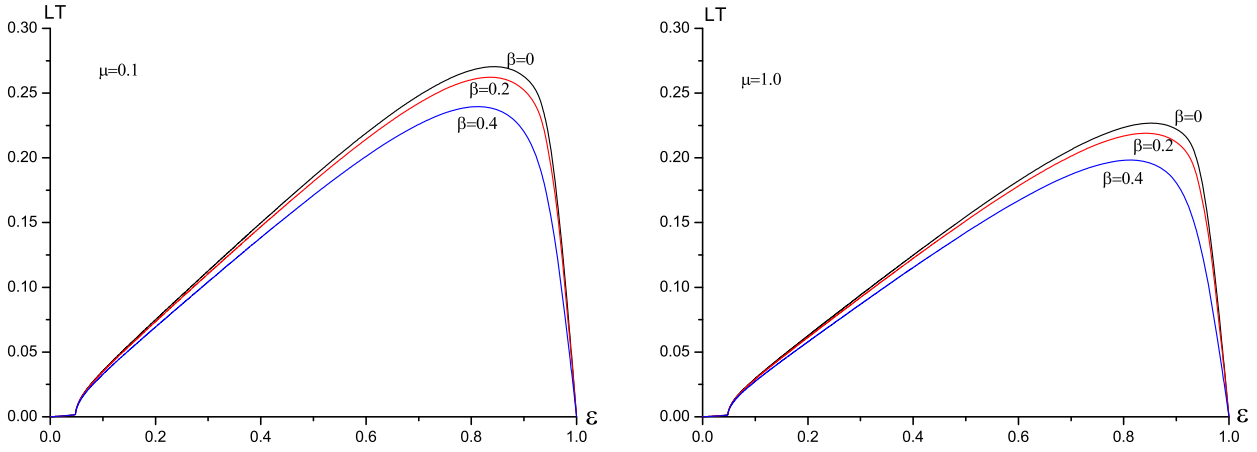

Fig. 3. LT versus ε for $\theta = \pi/2$. Left: $\mu = 0.1$. Right: $\mu = 1$. In all of the plots from top to bottom $\beta = 0, 0.2, 0.4$ respectively.

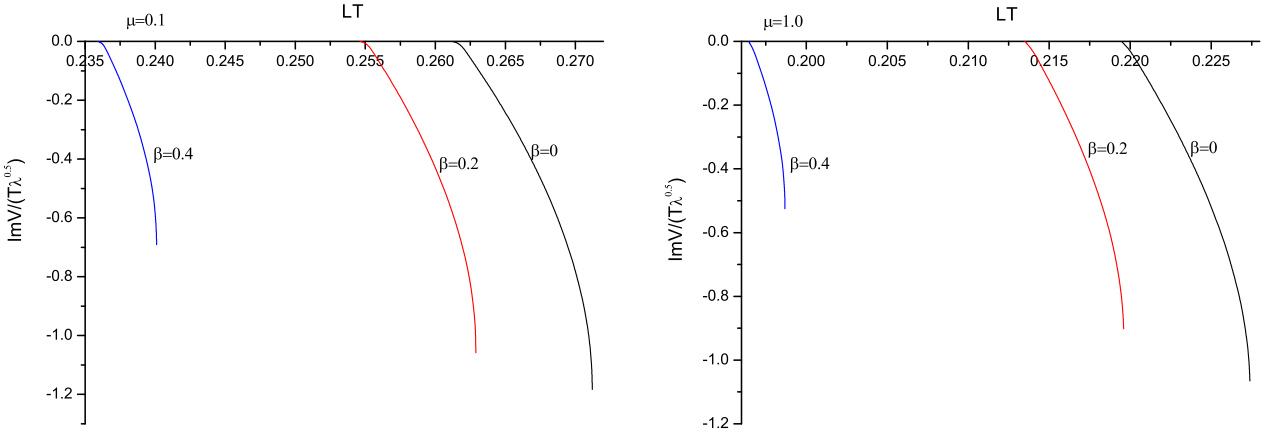

Fig. 4. $ImV/(\sqrt{\lambda}T)$ versus LT for $\theta = \pi/2$. Left: $\mu = 0.1$. Right: $\mu = 1$. In all of the plots from left to right $\beta = 0.4, 0.2, 0$ respectively.

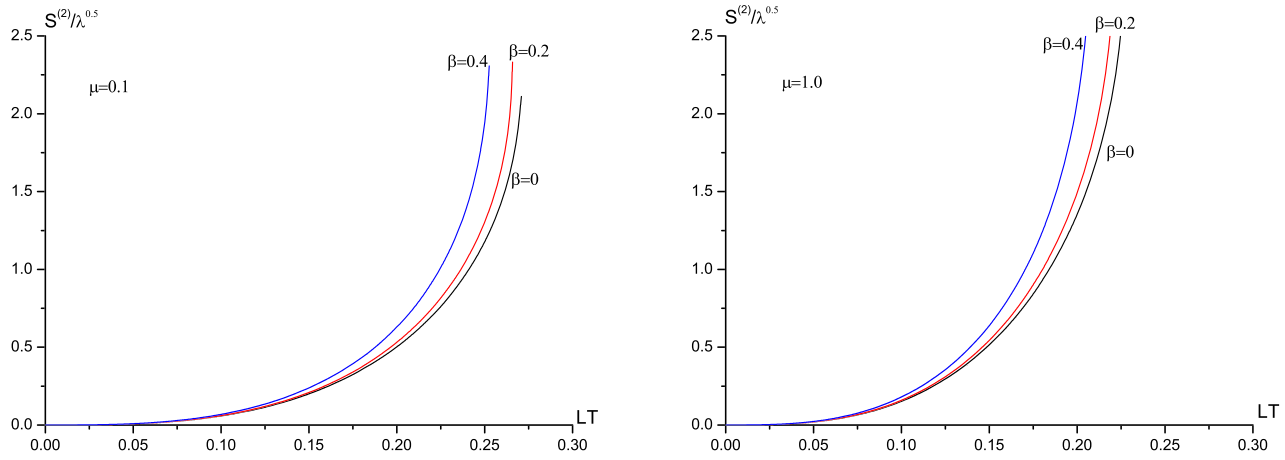

Fig. 5. $S^{(2)}/\sqrt{\lambda}$ versus LT for $\theta = 0$. Left: $\mu = 0.1$. Right: $\mu = 1$. In all of the plots from left to right $\beta = 0.4, 0.2, 0$ respectively.

case: At fixed chemical potential, increasing the rapidity leads to decreasing the absolute value of the imaginary potential; At fixed rapidity, increasing the chemical potential also leads to decreasing the absolute value of the imaginary potential. But one difference is that stronger modification occurs at $\theta = \pi/2$ than that at $\theta = 0$. In other words, the chemical potential has important effect when the quarkonium is moving transverse to the wind. This behavior is also similar to that of the higher derivative corrections [16].

We now conclude this section as follows:

1. The imaginary potential of the moving quarkonium depends on the chemical potential.
2. At fixed chemical potential, as the rapidity increases the absolute value of the imaginary potential decreases.
3. At fixed rapidity, as the chemical potential increases the absolute value of the imaginary potential decreases.
4. The chemical potential has a larger effect when the quarkonium is moving transverse to the wind than that parallel to the wind.
5. The presence of the chemical potential tends to decrease the thermal width or the dissociation length.

4. Entropic force

In this section, we analyze the chemical effect on the entropic force with respect to a moving quarkonium with the metric (6).

In [8], the entropic force is proposed to be related to the entropy S, that is

$$\mathcal{F} = T\frac{\partial S}{\partial L}, \tag{24}$$

where T is the temperature of the plasma, L refers to the interquark distance. Thus, to evaluate the entropic force, one needs to calculate these quantities: S, L and T, which have been studied from the AdS/CFT correspondence [32–34]. In this section, we follow the calculation of [27].

For the case of $\theta = 0$, the assumption and analysis are almost parallel to the previous section. From the Eq. (3) and Eq. (16), one finds

$$T = \frac{r_h}{\pi R^2}(1 - \frac{Q^2}{2}), \qquad L = 2\int_{r_c}^{\infty} dr \sqrt{\frac{a(r_c)b(r)}{a^2(r) - a(r)a(r_c)}}, \tag{25}$$

with

$$a(r_c) = \frac{r_c^4}{R^4}[f(r_c)sinh^4\beta + f(r_c)cosh^4\beta - sinh^2\beta cosh^2\beta(1 + f^2(r_c))],$$
$$f(r_c) = 1 - (1 + Q^2)(\frac{r_h}{r_c})^4 + Q^2(\frac{r_h}{r_c})^6. \tag{26}$$

and

$$a(r) = \frac{r^4}{R^4}[f(r)sinh^4\beta + f(r)cosh^4\beta - sinh^2\beta cosh^2\beta(1 + f^2(r))],$$
$$b(r) = cosh^2\beta - \frac{1}{f(r)}sinh^2\beta. \tag{27}$$

To study the entropy S, one can use the relation:

$$S = -\frac{\partial F}{\partial T}, \tag{28}$$

where F is the free energy of the $Q\bar{Q}$. Before studying the free energy, we should pause here to stress some issues. From the Fig. 1, we can see that for each plot LT has a maximum value. We call this value c. If $L > \frac{c}{T}$ the quarks are completely screened while $L < \frac{c}{T}$ the fundamental string is connected. Therefore, there are two cases for the free energy:

1. If $L > \frac{c}{T}$, the fundamental string will break in two pieces implying that the quarks are screened. In this case, the choice of the free energy $F^{(1)}$ is not unique [35], we here opt for a configuration of two disconnected trailing drag strings [36], that is

$$F^{(1)} = \frac{1}{\pi\alpha'}\int_{r_h}^{\infty} dr. \tag{29}$$

Applying (28), one finds

$$S^{(1)} = \sqrt{\lambda}\theta(L - \frac{c}{T}). \tag{30}$$

Note that c is a decreasing function of μ and β. One can obtain the value of c with numerical methods and also one can get it from the Fig. 1.

2. If $L < \frac{c}{T}$, the free energy of the $Q\bar{Q}$ can be derived from the on-shell action of the fundamental string in the dual geometry. Substituting (14) into (8), one gets

$$F^{(2)} = \frac{1}{\pi\alpha'}\int_{r_c}^{\infty} dr \sqrt{\frac{a(r)b(r)}{a(r) - a(r_c)}}. \tag{31}$$

Then using (28) one can calculate the entropy $S^{(2)}$ numerically. In Fig. 5, we plot $S^{(2)}/\sqrt{\lambda}$ versus LT at two different μ for various β. The left panel is plotted for $\mu = 0.1$ while the right one

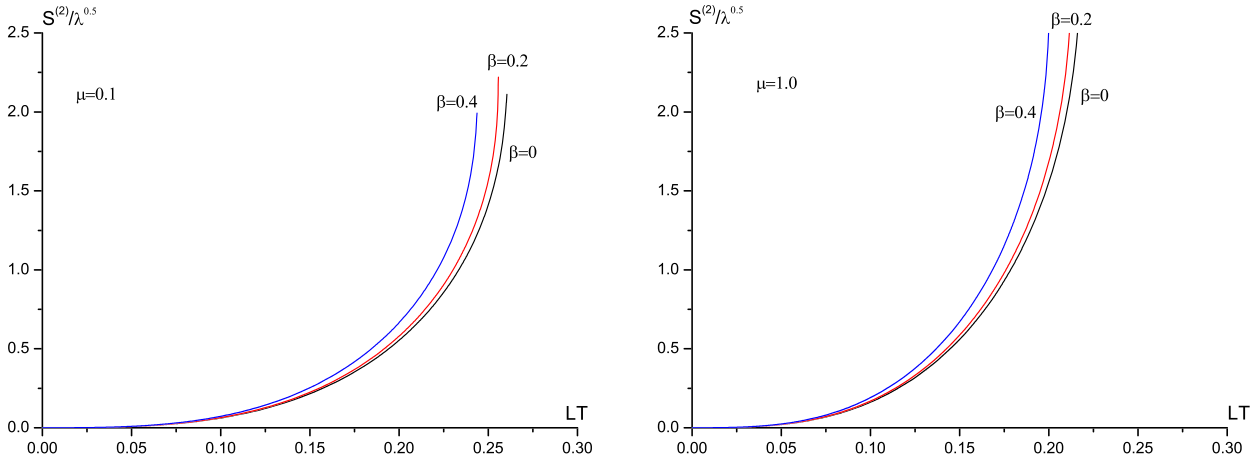

Fig. 6. $S^{(2)}/\sqrt{\lambda}$ versus LT for $\theta = \pi/2$. Left: $\mu = 0.1$. Right: $\mu = 1$. In all of the plots from left to right $\beta = 0.4, 0.2, 0$ respectively.

is plotted for $\mu = 1.0$. From the plots, we can see that at a fixed chemical potential by increasing the rapidity the entropy increases. This is consistent with that in [28]. In addition, to see the chemical effect, we compare the left panel with the right one and find that increasing μ leads to increasing the entropy. As stated above, the entropic force, responsible for dissociating the quarkonium, is related to the growth of the entropy with the distance. Therefore, increasing μ leads to increasing the entropic force or decreasing the dissociation length. Interestingly, the medium effect on the entropic force has also been studied in some other backgrounds [28]. The behavior there is similar.

For the case of $\theta = \pi/2$, we concern mainly with the final plots. In Fig. 6, we plot $S^{(2)}/\sqrt{\lambda}$ as a function of LT for $\theta = \pi/2$ at two chemical potential. We observe that the behavior is almost the same as the case of $\theta = 0$. The only difference is that μ has larger effect to the entropic force when the quarkonium is moving transverse to the wind comparing with the parallel motion.

We now conclude this section as follows:

1. The entropic force with respect to a moving quarkonium depends on the chemical potential.

2. At fixed chemical potential, as the rapidity increases the entropic force increases.

3. At fixed rapidity, as the chemical potential increases the entropic force increases.

4. The chemical potential has a larger effect to the entropic force when the quarkonium is moving transverse to the wind than that parallel to the wind.

5. The presence of the chemical potential tends to increase the entropic force or decrease the dissociation length.

5. Conclusion

In heavy ion collisions at LHC and RHIC, the quarkonium is usually moving through the sQQP with relativistic velocities. An understanding of how the quarkonium affected by the medium may be essential for theoretical predictions. Recently, the imaginary potential and the entropic force have been proposed to responsible for melting the heavy quarkonium respectively. The two quantities represent different mechanisms, so it is of interest to compare them. Evaluations of a same effect to these quantities could be considered as a simple comparison.

In this paper, we have investigated the chemical potential effect on the imaginary potential and the entropic force associated with a moving quarkina from the AdS/CTF duality. It is shown that for both mechanisms the chemical potential has the same effect: For the imaginary potential mechanism, the presence of the chemical potential tends to decrease the thermal width or decrease the dissociation length. For the entropic force mechanism, the chemical potential has the effect of increasing the entropic force or decreasing the dissociation length. In other words, for both mechanisms, it is found that the moving quarkonium dissociates easier at finite density.

However, the deep connection between the two mechanisms is still unknown. We hope to report our progress in this regard in future.

Acknowledgements

This research is partly supported by the Ministry of Science and Technology of the People's Republic of China (MSTC) under the "973" Project no. 2015CB856904(4). Zi-qiang Zhang and Gang Chen are supported by the NSFC under Grant no. 11475149. De-fu Hou is partly supported by the NSFC under Grant nos. 11375070 and 11524064.

References

[1] J. Adams, et al., STAR Collaboration, Nucl. Phys. A 757 (2005) 102.
[2] K. Adcox, et al., PHENIX Collaboration, Nucl. Phys. A 757 (2005) 184.
[3] E.V. Shuryak, Nucl. Phys. A 750 (2005) 64.
[4] Karen M. Burke, et al., JET Collaboration, Phys. Rev. C 90 (2014) 014909.
[5] T. Matsui, H. Satz, Phys. Lett. B 178 (1986) 416.
[6] M. Laine, O. Philipsen, P. Romatschke, M. Tassler, JHEP 03 (2007) 054.
[7] M.A. Escobedo, J. Phys. Conf. Ser. 503 (2014) 012026.
[8] D.E. Kharzeev, Phys. Rev. D 90 (2014) 074007.
[9] J.M. Maldacena, Adv. Theor. Math. Phys. 2 (1998) 231, Int. J. Theor. Phys. 38 (1999) 1113.
[10] S.S. Gubser, I.R. Klebanov, A.M. Polyakov, Phys. Lett. B 428 (1998) 105.
[11] O. Aharony, S.S. Gubser, J. Maldacena, H. Ooguri, Y. Oz, Phys. Rept. 323 (2000) 183.
[12] J. Noronha, A. Dumitru, Phys. Rev. Lett. 103 (2009) 152304.
[13] S.I. Finazzo, J. Noronha, JHEP 11 (2013) 042.
[14] K.B. Fadafan, D. Giataganas, H. Soltanpanahi, JHEP 11 (2013) 107.
[15] M. Ali-Akbari, D. Giataganas, Z. Rezaei, Phys. Rev. D 90 (2014) 086001.
[16] K.B. Fadafan, S.K. Tabatabaei, J. Phys. G: Nucl. Part. Phys. 43 (2016) 095001.
[17] D. Giataganas, arXiv:1306.1404v3 [hep-th].
[18] J. Sadeghi, S. Tahery, JHEP 06 (2015) 204.
[19] J. Sadeghi, S. Tahery, arXiv:1509.01309 [hep-th].
[20] J.L. Albacete, Y.V. Kovchegov, A. Taliotis, Phys. Rev. D 78 (2008) 115007.
[21] T. Hayata, K. Nawa, T. Hatsuda, Phys. Rev. D 87 (2013) 101901.
[22] K.H. Meyer, G. Susich, E. Valk, Kolloid Z. 59 (1932) 208.
[23] E.P. Verlinde, On the origin of gravity and the laws of Newton, JHEP 04 (2011) 029.
[24] O. Kaczmarek, F. Karsch, P. Petreczky, F. Zantow, Phys. Lett. B 543 (2002) 41.
[25] O. Kaczmarek, F. Zantow, arXiv:hep-lat/0506019.
[26] P. Petreczky, K. Petrov, Phys. Rev. D 70 (2004) 054503, arXiv:hep-lat/0405009.
[27] K. Hashimoto, D.E. Kharzeev, Phys. Rev. D 90 (12) (2014) 125012.
[28] K.B. Fadafan, S.K. Tabatabaei, Phys. Rev. D 94 (2016) 026007.

[29] Z-q. Zhang, C. Ma, D-f. Hou, G. Chen, arXiv:1611.08011 [hep-ph].
[30] E.D. Hoker, D.Z. Freedman, arXiv:hep-th/0201253.
[31] D. Bak, A. Karch, L.G. Yaffe, JHEP 0708 (2007) 049.
[32] J.M. Maldacena, Phys. Rev. Lett. 80 (1998) 4859.
[33] A. Brandhuber, N. Itzhaki, J. Sonnenschein, S. Yankielowicz, Phys. Lett. B 434 (1998) 36.
[34] S.-J. Rey, S. Theisen, J.-T. Yee, Nucl. Phys. B 527 (1998) 171.
[35] M. Chernicoff, J.A. Garcia, A. Guijosa, JHEP 09 (2006) 068.
[36] C.P. Herzog, A. Karch, P. Kovtun, C. Kozcaz, L.G. Yaffe, JHEP 07 (2006) 013.